Tokamak equilibrium

Youwen Sun
ywsun@ipp.ac.cn

Institute of plasma physics, Chinese Academy of Sciences

Chinese Summer School on Plasma Physics
Jul. 7-12, 2025, USTC, Hefei

Contents

Contents

Magnetically confined fusion

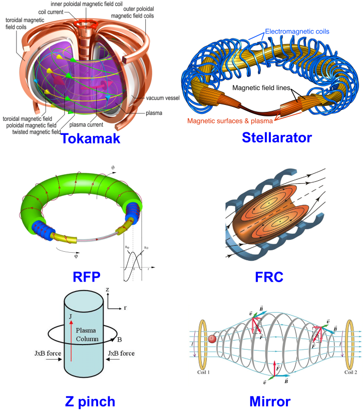

1.1 Fusion configurations

- **Toroidal** configurations ⇒ suppress the loss cone
- **Rotational transform** [$\iota = 1/q$, where q is safety factor] ⇒ reduce direct drift orbit loss
  - Non-axisymmetric magnetic configurations employ **external coils** to generate ι
  - Axisymmetric machines use the **toroidal plasma current**
- **Tokamak** achieved the highest performance $nT\tau_E$

Tokamak magnetic field configuration

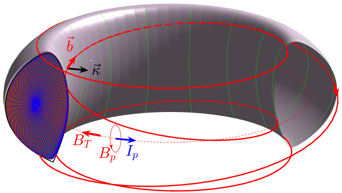

1.2 Tokamak

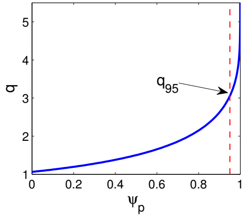

1.3 q profile

- Magnetic field can be represented as

$$\begin{aligned}\vec{B} =&\nabla\psi_t \times \nabla\theta - \nabla\psi_p \times \nabla\zeta \\ =&\nabla\phi \times \nabla\psi_p + g\nabla\phi,\end{aligned} \quad (1)$$

  where ϕ is the geometric toroidal angle. Here $|\nabla\psi_p| = RB_p$ and $g(\psi_p) = B_\zeta = RB_T$. It has $B_p/B_T \sim O(\epsilon)$, and $\epsilon = a/R_0$ with R_0 and a are major and minor radii, respectively.

- Rotational transform ⇒ nested magnetic **flux surfaces**
  - **Rational** or **resonant surface** $q \equiv \frac{d\psi_t}{d\psi_p} = m/n$, where m and n are toroidal and poloidal turns
  - Edge safety factor, q_{95}, is defined as the safety factor at $\hat{\psi}_p = 0.95$ (0 at center, 1 at boundary)

Characteristics of Divertor configuration

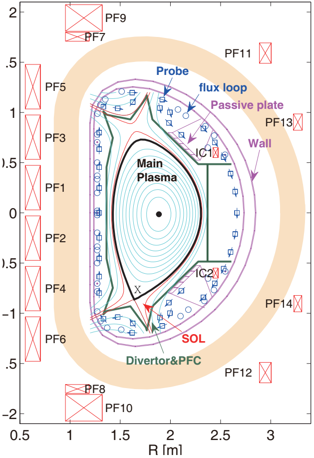

1.4 EAST configuration

- Nested closed magnetic flux surfaces inside the last closed flux surface (**LCS**)
  $\Rightarrow$ confinement area
- A thin layer (1-2 cm) just outside the LCS is called scrape-off layer (**SOL**)
  $\Rightarrow$ open field lines cause the particles and heat flux toward the Divertor
- On **separatrix** between the LCS and SOL, there is a point (or multiple points) with $B_p = 0$ called **X point**
- Approaching the LCS, it has $q \to \infty$

MHD momentum equation

Momentum equation from a single fluid model can be written as

$$\rho_m \frac{d}{dt}\vec{V} = \vec{J}\times\vec{B} - \nabla P - \nabla\cdot \overleftrightarrow{\Pi} + \vec{S}_M + O, \qquad (2)$$

where $\frac{d}{dt} \equiv \frac{\partial}{\partial t} + \vec{V}\cdot\nabla$.

- Left hand side: **inertial terms**. $\vec{V}\cdot\nabla$ is the **advection term** that counts the non-inertial force and non-linear effect.
- Right hand side. First two terms: **Compressed Alfven wave** with a characteristic time $\tau_{CA} \sim 10^{-7}$s. Without **pressure anisotropy**, the rest terms describe the **momentum dissipation** in a time scale of momentum confinement time, $\tau_M \sim \tau_E \sim 10^{-1}$s.

$$\frac{\partial^2}{\partial t^2}\vec{\xi}_\perp \approx (1+\beta)V_A^2\nabla_\perp\left(\nabla_\perp\cdot\vec{\xi}_\perp\right), \qquad (3)$$

- In the limit $\tau_{CA} \ll \tau \ll \tau_M$, with negligible pressure anisotropy and $V \ll C_S$, the leading terms (black part in Eq. (2)) forms the force balance equation.

Ideal MHD force balance equation

Force balance equation

$$\boxed{\vec{J} \times \vec{B} - \nabla P = 0.} \tag{4}$$

- Thermal expansion ⇔ Lorenz force
- Pressure is a flux function, $\vec{B} \cdot \nabla P = 0$. Current is lying on the flux surface. Only perpendicular current contribute to the force balance. It has

$$\vec{J}_\perp = -J_\perp \frac{1}{B} \vec{b} \times \nabla \psi_p \tag{5}$$

  where $J_\perp = -\frac{\mathrm{d}P}{\mathrm{d}\psi_p}$.
- It can also be rewritten as

$$\nabla_\perp (P + \frac{B^2}{2\mu_0}) = \frac{B^2}{\mu_0} \vec{\kappa}, \tag{6}$$

  where $\vec{\kappa} \equiv \vec{b} \cdot \nabla \vec{b}$ is the curvature of the field line and $\nabla_\perp = \nabla - \vec{b}\vec{b} \cdot \nabla$.

Radial force balance equation

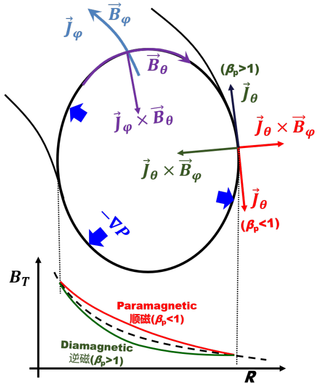

1.5 Force balance

Radial force balance can be rewritten as

$$e_\psi\cdot\left(\vec{J}\times\vec{B}-\nabla P\right)$$
$$=-\frac{1}{B^\theta}\left(J^\phi B^\theta-B^\phi J^\theta\right)-\frac{\mathrm{d}P}{\mathrm{d}\psi_p}=0. \qquad (7)$$

- $-\nabla P$: Outward
- Toroidal current: Inward
- Poloidal current: depends on the orientation of the current. It has

$$\beta_p\equiv\frac{2\mu_0\langle P\rangle_V}{\left\langle B_p^2\right\rangle_{lcs}}\approx 1-\left(\frac{1+\kappa^2}{2\kappa}\right)\frac{8\pi B_{T0}}{(\mu_0 I_p)^2}\delta\Phi\sim O(1), \qquad (8)$$

where the **diamagnetic toroidal flux** $\delta\Phi$ can be measured from diamagnetic loop.

- Internal inductance: $l_i\equiv\frac{\langle B_p^2\rangle_V}{\langle B_p\rangle_S^2}$
- Total beta: $\beta_T\equiv 2\mu_0\langle P\rangle_V/B_0^2\propto\frac{\epsilon^2}{q_{95}^2}\beta_p\sim O(1\%)$
- Normalized beta: $\beta_N\equiv\beta_T[aB/I_p]\sim O(1)[\%\mathrm{m}\cdot\mathrm{T/MA}]$

Grad-Shafralov equation

- Using Eq. (1) for axisymmetric case, the radial force balance equation (7) can also be written as **Grad-Shafralov** equation [Grad, **JNE 7**, 284 (1958)], [Shafranov, **JETP 6**, 545 (1958)]

$$\boxed{\triangle^* \psi_p(R,Z) = -\mu_0 R^2 P' - gg',} \tag{9}$$

where $\triangle^* \equiv R^2 \nabla \cdot (\frac{1}{R^2}\nabla) = R\frac{\partial}{\partial R}(\frac{1}{R}\frac{\partial}{\partial R}) + \frac{\partial^2}{\partial Z^2}$, $P' \equiv \frac{\mathrm{d}P}{\mathrm{d}\psi_p}$ and $g' \equiv \frac{\mathrm{d}g}{\mathrm{d}\psi_p}$.

- There are 3 unknown profiles
  - left: **toroidal current**, $\triangle^* \psi_p(R,Z) = \mu_0 J_\phi$
  - 1^{st} term on the RHS : plasma pressure or **perpendicular current**, $J_\perp = -J^\alpha = -\frac{\mathrm{d}P}{\mathrm{d}\psi_p}$
  - 2^{nd} term on the RHS : **poloidal current**, $\frac{\mathrm{d}g}{\mathrm{d}\psi_p} = -\mu_0 \frac{J^\theta}{B^\theta}$
- It is only possible to get one unique solution with the knowledge at least 2 of them.
- P and g are flux function, while $J_\phi = R^2 J^\phi$ is not.
- Here $F^\phi = \vec{F} \cdot \nabla\phi$ and $F^\theta = \vec{F} \cdot \nabla\theta$ are the contravariant components of the field.

Contents

Solution of the G-S equation

- Analytic solution with assumption of either simple current profiles or simple geometry (for instance, circular shaped plasma with large aspect ratio, or Solov's solution for general geometry but constant current profiles)
- Equilibrium solution with prescribed boundary and kinetic profiles (P', gg') can be numerically solved
- Equilibrium reconstruction $\psi_p(R, Z)$ by using least square fitting of experimental measurements
  - Current filaments method, which represents plasma as several current filaments
  - Fitting method (e.g. EFIT), which represents the current profiles as truncated polynomial functions

Analytic solution for shift circle equilibrium

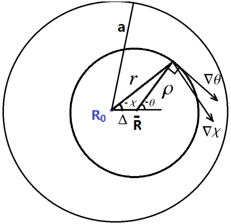

1.6 Shift circle

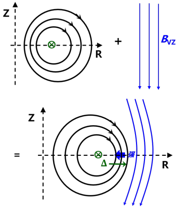

Writing the flux surface position as

$$R = R_0 + r\cos(\chi) + \Delta_{GS}, \tag{10a}$$

$$Z = Z_0 - r\sin(\chi), \tag{10b}$$

where Δ_{GS} is the **Grad-Shafranov shift** [Shafranov, **JNE 5**, 251 (1963)] , [Mukhovatov, **NF 6**, 605 (1971)] , it has $\psi_p \approx \psi_{p0}(r) - \psi'_{p0}\Delta_{GS}\cos\chi$.

The order with $\cos\chi$ in G-S equation becomes

$$\frac{1}{f^2}\left(rf^2\Delta'_{GS}\right)' = -\left(\alpha_p + \epsilon\right), \tag{11}$$

with $f = \frac{\psi'_{p0}}{R_0B_0} \approx \frac{\epsilon}{q}$, $\epsilon = \frac{r}{R_0}$ and $\alpha_p \equiv -q^2R\beta'$.

The solution can be written as

$$\Delta'_{GS}(r) = -\epsilon\left(\Lambda + 1\right), \tag{12}$$

where $\Lambda \equiv \beta_p + \frac{1}{2}l_i - 1$.

The external **vertical field** is approximately

$$\vec{B}_v \approx -\frac{\mu_0 I_p}{4\pi R_0}\left[\ln\frac{8R_0}{a} + \Lambda - \frac{1}{2}\right]\vec{e}_Z. \tag{13}$$

Plasma Shaping

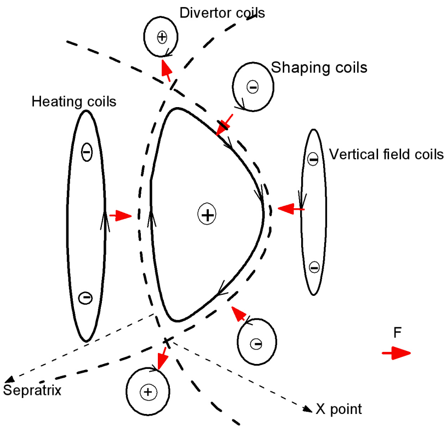

1.8 Forces for shaping

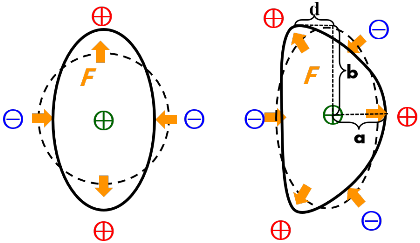

1.9 plasma shaping

- **Quadrupole field** makes elongation $\kappa = b/a$, and **hexapole field** makes triangularity $\delta = d/a$.
- Analytic **Solov's solution** for **general shape** but constant current profile has been developed [Cerfon, **PoP 17**, 032502(2010)]
- Miller equilibrium [Miller, **PoP 5**, 973 (1998)]

Vertical instability

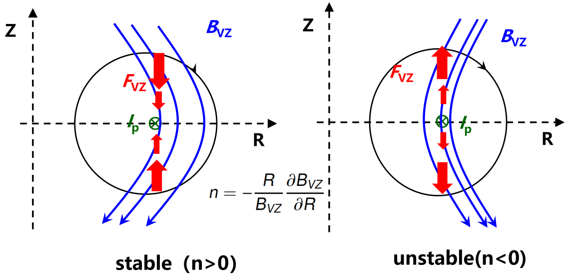

1.10 VDE

- Vertical motion can be unstable for certain applied vacuum vertical field
- Stability depends on the index of field decay: $n \equiv -\frac{R}{B_{VZ}}\frac{\partial B_{VZ}}{\partial R}$
- **Vertical displacement event** (VDE) can be triggered by elongation

EFIT reconstruction – Fitting toroidal current profile

- Iteration method with an initial guess of $\psi_p = \psi_{p,0}$ is used to solve this non-linear second order differential equation.
- The terms P' and gg' are represented by some truncated base functions of ψ_p [Lao, **NF 25**, 1611 (1985)]

$$P' \equiv \sum_{m=0}^{M} \alpha_m \Phi_m(\psi_p) \quad and \quad gg' \equiv \sum_{n=0}^{N} \beta_n \Phi_n(\psi_p). \tag{14}$$

At the step l, the coefficients α_{ml} and β_{nl} , and hence the toroidal current profile, are determined by minimization

$$\chi^2 = \frac{1}{k} \sum_{j=1}^{k} \frac{[\psi^*_{ps,j} - \psi^c_{ps,j}(\alpha_m, \beta_n)]^2}{\sigma_j^2}, \tag{15}$$

where

$$\psi^c_{ps,j} = \int G_{ps,j} J_t(\alpha_{ml}, \beta_{nl}, \psi_{p,l-1}) ds_\phi + \sum_i G_{exs,ij} I_i^{ex}, \tag{16}$$

and $\psi^*_{ps,j}$ is measured value of the j^{th} sensor.

EFIT reconstruction – G-S solution

The poloidal flux distribution can be found by using one of the following two methods:

- Green function method.
  the poloidal flux ψ_p at the j^{th} grid point of the calculation area (R, Z) at this step can be upgraded from

$$\psi_{p,l,j} = \int G_{pp,j} J_t(\alpha_{ml}, \beta_{nl}, \psi_{p,l-1}) ds_\phi + \sum_i G_{exp,ij} I_i^{ex} \tag{17}$$

- Solving the second order differential equation

$$\triangle^* \psi_p(R, Z) = \mu_0 R J_t \tag{18}$$

The newly obtained poloidal flux replaces the initial one and the whole process is repeated until it converges.

Diagnostics required for equilibrium reconstruction

- **External magnetic diagnostics**.
  For instance, **flux loops**, **saddles** and **magnetic pick-up probes** *etc*. which can accurately determine the plasma edge flux profile. It produces mainly the information about the total toroidal plasma current.
- **Intermal magnetic measurement**
  With the constraints from the internal magnetic measurements, for instance, **MSE** and **polarization interferometer**, more accurate toroidal plasma current profile near the core can be obtained.
- **Diamagnetic measurement**
  produce information about the total internal poloidal current g'.
- **Kinetic profiles**
  Plasma density and temperature profiles from for instance **TS** and **CXRS**, gives the constraints on the plasma pressure gradient. The neoclassical **Bootstrap current** evaluated from these kinetic profiles can be further used for the constraints on the flux averaged parallel plasma current.
- **Others**
  Soft-X-Ray and **ECE** etc produce the information about the positions sawtooth inversion radius, and other high m perturbations etc.

Examples of equilibrium Solutions

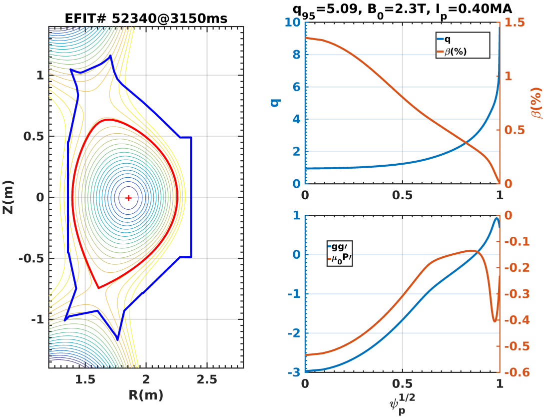

1.11 EFIT outputs [Lao, **NF 25**, 1611 (1985)]

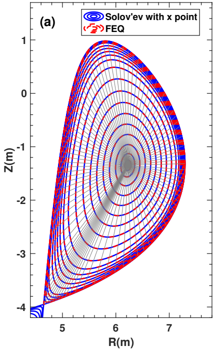

1.12 FEQ solution [Jiang, **PST 24**, 015105 (2022)]

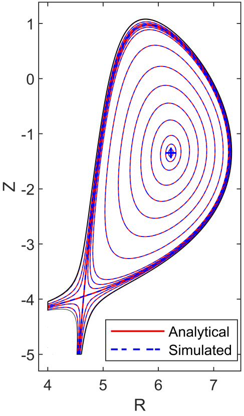

1.13 FDEQ solution [Dong, **CPC 315**, 109715(2025)]

3D equilibrium in tokamaks

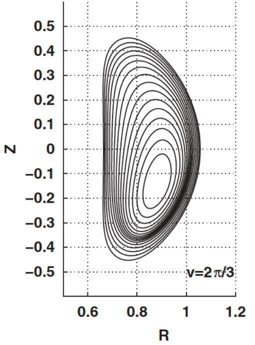

1.14 Helical core by VMEC/ANIMEC [Cooper, **PRL 105**, 035003 (2010)]

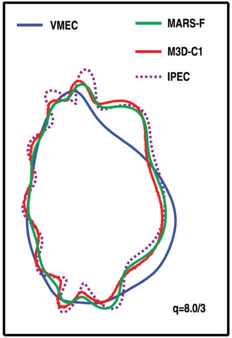

1.15 3D from RMP [Turnbull, **PoP 20**, 056114 (2013)]

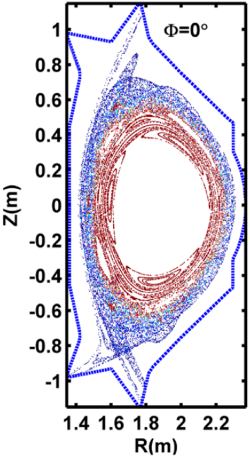

1.16 Edge stochastic field [Jia, **PPCF 58**, 055010 (2016)]

Contents

Flux coordinates

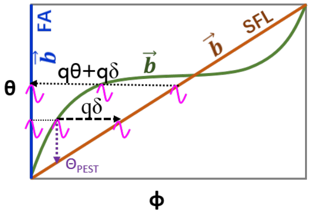

1.17 Flux coordinates and field aligned coordiantes

- In **flux coordinates** (ρ, θ, ζ), the magnetic field can be written as

$$\begin{aligned} \vec{B} &= \nabla\psi_t \times \nabla\theta - \nabla\psi_p \times \nabla\zeta \\ &= \psi_p'[q\nabla\rho \times \nabla\theta - \nabla\rho \times \nabla\zeta], \end{aligned} \quad (19)$$

where prime denotes the derivative over ρ.
Since $\vec{B} \cdot \nabla(q\theta - \zeta) = 0$, it is also known as **straight field line coordinates** [Dhaeseleer, "Flux Coordinates and Magnetic Field Structure", **Springer**,(1991)].

- Using the **field aligned coordinates** $(\rho, \alpha = q\theta - \zeta, \theta)$, it is obvious that

$$\vec{B} \cdot \nabla = B^\theta \partial_\theta, \quad (20)$$

and the Jacobian of (ρ, α, θ) can be written as
$\mathcal{J}^{-1} \equiv (\nabla\rho \times \nabla\alpha) \cdot \nabla\theta = (\nabla\rho \times \nabla\theta) \cdot \nabla\zeta = B^\theta/\psi_p'$.

Choices of flux coordinates

- Radial coordinates. $\rho = \rho(\psi)$, such as ψ_p, ψ_t, $V(\psi)$, $q(\psi)$ etc, e. g. $\rho = \rho_t \equiv \sqrt{\frac{2\psi_t}{B_0}}$.
- Other two angle-like coordinates can have different choices [Sun, **PPCF 57**, 045003 (2015)]
  - θ is chosen for a given form of Jacobian $\mathcal{J}^{-1} \equiv (\nabla\rho \times \nabla\theta) \cdot \nabla\zeta = \frac{B_p}{|\psi_p'|} \left.\frac{\partial\theta}{\partial l}\right|_{\psi_p,\phi}$ via

$$\left.\frac{\partial\theta}{\partial l}\right|_{\psi_p,\phi} = \frac{|\psi_p'|}{\mathcal{J}B_p}, \tag{21}$$

    where prime denotes derivative over ρ.
  - toroidal angle like coordinate can be often chosen as

$$\zeta \equiv \phi - q(\psi_p)\delta(\psi_p, \theta), \tag{22}$$

    where ϕ is the geometric toroidal angle of the machine, (R, ϕ, Z) is a cylindrical coordinates, δ is a periodic function of θ. It can be evaluated from

$$\partial_\theta\delta = \frac{g\mathcal{J}}{qR^2}\frac{1}{\psi_p'} - 1. \tag{23}$$

The form of $\mathcal{J}$

- For a given form of $\mathcal{J}_0$ and writing
$$\mathcal{J} = \hat{V}'\mathcal{J}_0 \langle 1/\mathcal{J}_0 \rangle_\psi , \tag{24}$$
the flux coordinates can be obtained by integrating Eqs. (21) and (23) over the poloidal contour of the flux surface. Here $\langle ... \rangle_\psi$ denotes flux average, $\hat{V} = V/(4\pi^2)$, $V(\psi_p)$ is the volume enclosed by the flux surface.
- For example, if we define
$$\mathcal{J}_0 \equiv \frac{R^i}{|\nabla\psi_p|^j B^k} \tag{25}$$
and give a group of values of (i, j, k) one flux coordinates can be obtained.
- The safety factor can be evaluated from
$$q(\psi_p) \equiv \frac{1}{2\pi}\oint \frac{B^\zeta}{B^\theta} d\theta = \frac{\hat{V}'}{\psi_p'} g \left\langle 1/R^2 \right\rangle_\psi . \tag{26}$$

Frequently used flux coordinates

The most often used straight field line coordinates are listed in the following.

- **PEST coordinates:**
  If $i = 2,\ j = k = 0$, the coordinates will be PEST coordinates. It has $\mathcal{J}_0 = R^2$, $\zeta = \phi$ and $\mathcal{J} = \hat{V}' < 1/R^2 >_\psi R^2 = \hat{V}' < B_t^2 >_\psi /B_t^2$. It is also named as the basic straight field line coordinates.
- **Hamada coordinates:**
  If $i = j = k = 0$, the coordinates will be Hamada coordinates. It has $\mathcal{J}_0 = 1$, and $\mathcal{J} = \hat{V}'$.
- **Boozer coordinates:**
  If $i = 0,\ j = 0,\ k = 2$, the coordinates will be Boozer coordinates. It has $\mathcal{J}_0 = 1/B^2$, and $\mathcal{J} = \hat{V}' < B^2 >_\psi /B^2$.
- **Equal-arc coordinates:**
  If $i = j = 1,\ k = 0$, the coordinates will be Equal-arc coordinates. It has $\mathcal{J}_0 = 1/B_p$, $\partial_l \theta|_{\psi_p,\phi} = 2\pi/l$, and $\mathcal{J} = \hat{V}' < B_p >_\psi /B_p$.

Example of flux coordinates

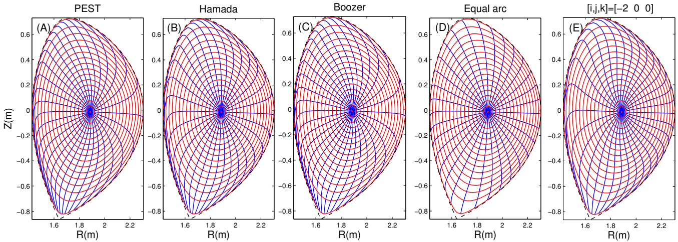

1.18 Examples for EAST equilibrium [Sun, **PPCF 57**, 045003 (2015)]

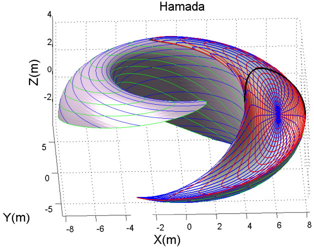

1.19 3D view of constant ζ grids

Geometric properties and their relations

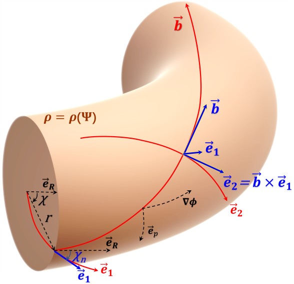

1.20 $(\vec{e}_1 = \vec{e}_n, \vec{e}_2 = \vec{b} \times \vec{e}_1, \vec{b})$

[Sun, **AIP advances 14**, 055206 (2024)]

$$\vec{e}_2 \equiv \vec{b} \times \vec{e}_n = -\frac{1}{\lambda R}\left(R^2\nabla\phi - \frac{g}{B}\vec{b}\right)$$
$$= \lambda R \nabla_s \alpha, \tag{27}$$

where $\nabla_s = \nabla - \vec{e}_1\vec{e}_1 \cdot \nabla$, and $\lambda \equiv \frac{B_p}{B} = \psi_p' \frac{|\nabla\rho|}{RB}$.

- **Curvature** of field line can be written as

$$\vec{\kappa} = \vec{b} \cdot \nabla\vec{b} \equiv \kappa_n \vec{e}_1 + \kappa_g \vec{e}_2 = \frac{\mu_0}{B^2}\nabla_\perp\left(P + \frac{B^2}{2\mu_0}\right) \approx \frac{1}{B}\nabla_\perp B. \tag{28}$$

Another important curvature is κ_ρ defined as

$$\kappa_\rho \equiv \vec{\kappa} \cdot e_\rho = \frac{1}{|\nabla\rho|}\left(\kappa_n - \kappa_g \bar{\Lambda}_0\right) \approx -\frac{1}{R_0}\left[\cos\theta + \sin\theta\left(s\theta - \alpha_p \sin\theta\right)\right], \tag{29}$$

where $\bar{\Lambda}_0 \equiv \frac{\vec{e}_1 \cdot \nabla\alpha}{\vec{e}_2 \cdot \nabla\alpha} \approx \Lambda_0 \equiv s\theta - \alpha_p \sin\theta$, $s \equiv \frac{\rho}{q}q'$ is the global magnetic shear, and $\alpha_p \equiv -q^2 R\beta'$. It has $\kappa_n \approx -\frac{\cos\theta}{R}$ and $\kappa_g \approx \frac{\sin\theta}{R}$.

- **Torsion** of field line can be written as

$$\tau_n \equiv -\vec{e}_1 \cdot \left(\vec{e}_2 \cdot \nabla\vec{b}\right) \tag{30}$$

- **Local magnetic shear**

$$s_1 \equiv \vec{e}_2 \cdot \nabla \times \vec{e}_2 \approx \vec{b} \cdot \nabla\bar{\Lambda}_0 \approx \vec{b} \cdot \nabla\left(s\theta - \alpha_p \sin\theta\right). \tag{31}$$

It has $\sigma \equiv \frac{\mu_0 J_\parallel}{B} = s_1 + 2\tau_n$, and $\vec{b} \cdot \nabla\sigma = \vec{b} \cdot \nabla\sigma_{ps} = \kappa_g |\nabla\rho| \frac{2\mu_0 P'}{B^2}$.

Example of Geometric properties

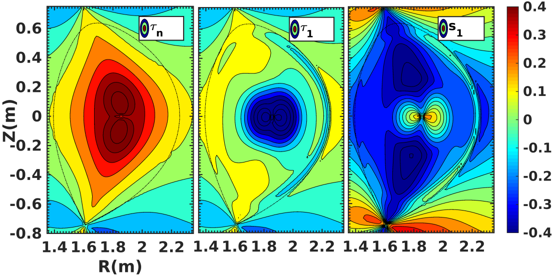

1.21 Some geometric properties [Sun, **AIP advances 14**, 055206 (2024)]

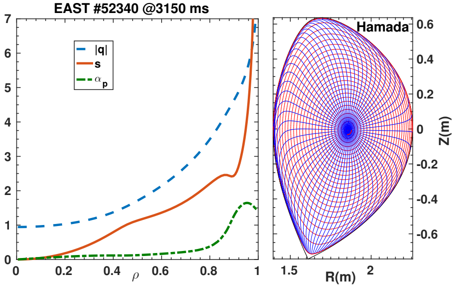

1.22 EAST 52340 [Sun, **PoP 26**, 072504 (2019)]

Vector representation and differential operators

- Any vector field can be expressed as $\vec{A} \equiv A^i e_i \equiv A_i e^i$. Here $A_i = \vec{A} \cdot e_i$ and $A^i = \vec{A} \cdot e^i$ are the **covariant** and **contravariant** parts of the vector, respectively. It has $A_i = g_{ij} A^j$, $A^i = g^{ij} A_j$.
- Usually, either e^i or e_i is not a unit vector. Therefore, both the covariant and contravariant parts of the vector are different from the physical values in the corresponding direction.
- The gradient, divergence, curl and Laplacian can be written as

$$\nabla f = \nabla\alpha \frac{\partial}{\partial\alpha} f, \tag{32a}$$

$$\nabla \cdot \vec{V} = \mathcal{J}^{-1} \frac{\partial}{\partial\alpha}(\mathcal{J} V^{\alpha}), \tag{32b}$$

$$\nabla\gamma \cdot (\nabla \times \vec{V}) = \mathcal{J}^{-1}\left(\frac{\partial}{\partial\alpha} V_{\beta} - \frac{\partial}{\partial\beta} V_{\alpha}\right), \tag{32c}$$

$$\nabla^2 f = \nabla \cdot \nabla f = \mathcal{J}^{-1} \frac{\partial}{\partial\alpha}\left(\mathcal{J} g^{\alpha\beta} \frac{\partial}{\partial\beta} f\right). \tag{32d}$$

Example of reduced differential operators

- For $k_\parallel \ll k_\perp$, it has

$$\nabla\cdot\vec{F} \xrightarrow{\vec{F}_\perp\equiv\frac{\vec{B}\times\nabla f}{B^2}} B\nabla_\parallel(F_\parallel/B)+\mathcal{K}(f), \tag{33a}$$

$$\nabla_\parallel f \approx \frac{G_\parallel}{qR_0}\partial_\theta f - \frac{qB}{\rho B_0}\{\tilde{A}/B, f\}_{\rho\alpha}, \tag{33b}$$

$$\nabla_\perp^2 f \approx \frac{G}{\rho}\partial_\rho\left[\frac{\rho}{G}(g^{\rho\rho}\partial_\rho + g^{\rho\alpha}\partial_\alpha)\right]f + \partial_\alpha\left[(g^{\rho\alpha}\partial_\rho + g^{\alpha\alpha}\partial_\alpha)\right]f, \tag{33c}$$

$$\vec{V}_E\cdot\nabla f \equiv \frac{\vec{B}\times\nabla\Phi}{B^2}\cdot\nabla f \approx \frac{q}{\rho B_0}\{\Phi, f\}_{\rho\alpha}, \tag{33d}$$

$$\mathcal{K}(f) \equiv \nabla\cdot\left(\frac{\vec{B}\times\nabla f}{B^2}\right) \approx \frac{q}{\rho B_0 B^2}\left[\partial_\rho B^2\partial_\alpha f - \frac{RG_\parallel}{qR_0}\partial_\theta B^2\partial_\rho f\right], \tag{33e}$$

where the Poison bracket $\{A, B\}_{\rho\alpha} = \partial_\rho A\partial_\alpha B - \partial_\alpha A\partial_\rho B$, $G \equiv g\left\langle 1/R^2\right\rangle_\psi$, and $G_\parallel \equiv \frac{RR_0\langle 1/R^2\rangle_\psi}{\mathcal{J}_0\langle 1/\mathcal{J}_0\rangle_\psi} \approx 1$.

- Shift metric method [Scott, **PoP 8**, 447 (2001)] , $\alpha \to \alpha_k = q(\theta-\theta_k) - \zeta + \delta_k(\rho)$ so that $g^{\rho\alpha_k}|_{\theta=\theta_k} = 0$, is necessary to conquer the difficulty in the evaluation of radial derivative, and it has $\nabla_\perp^2 f \approx \frac{G}{\rho}\partial_\rho[\frac{\rho}{G}(g^{\rho\rho}\partial_\rho)]f + \frac{q^2}{\rho^2}\partial_{\alpha_k}^2 f$.

An alternative method using geometric properties

Using geometric properties [Sun, **AIP advances 14**, 055206 (2024)], the fundamental differential operators can also be rewritten as

- Divergence

$$\nabla\cdot\vec{F}=\sum_{j=1}^{3}\left(\vec{e}_j\cdot\nabla F_j\right)-\left(\kappa_{nd}+\kappa_n\right)F_1 -\left(\hat{g}\kappa_p+\kappa_g\right)F_2-\frac{\lambda}{\hat{g}}\kappa_g F_3, \tag{34}$$

where $\hat{g}=g/(RB)$.

- Directional derivative

$$\vec{e}_i\cdot\nabla\vec{F}=\left(M_d+\mathcal{I}\vec{e}_i\cdot\nabla\right)\begin{pmatrix}F_1\\F_2\\F_3\end{pmatrix}, \tag{35}$$

where $M_d=\begin{pmatrix}0 & -\vec{b}\cdot\vec{d}_i & \vec{e}_2\cdot\vec{d}_i\\ \vec{b}\cdot\vec{d}_i & 0 & -\vec{e}_1\cdot\vec{d}_i\\ -\vec{e}_2\cdot\vec{d}_i & \vec{e}_1\cdot\vec{d}_i & 0\end{pmatrix}$, and

$\vec{d}_i=\vec{e}_i\times\vec{\kappa}_i+\tau_i\vec{e}_i$, $\vec{\kappa}_i\equiv\vec{e}_i\cdot\nabla\vec{e}_i$, and
$\tau_i\equiv\delta_{ijk}\left(\vec{e}_i\cdot\nabla\vec{e}_j\right)\cdot\vec{e}_k$.

- Curl

$$\nabla\times\vec{F}=\left(\mathcal{R}^T+M_c\right)\begin{pmatrix}F_1\\F_2\\F_3\end{pmatrix}, \tag{36}$$

where $\mathcal{R}=\begin{pmatrix}0 & -\lambda\kappa_p & \hat{g}\kappa_p\\ \kappa_{bd} & s_1 & -\kappa_{nd}\\ -\kappa_g & \kappa_n & \sigma\end{pmatrix}$, and

$$M_c=\begin{pmatrix}0 & -\vec{b}\cdot\nabla & \vec{e}_2\cdot\nabla\\ \vec{b}\cdot\nabla & 0 & -\vec{e}_1\cdot\nabla\\ -\vec{e}_2\cdot\nabla & \vec{e}_1\cdot\nabla & 0\end{pmatrix}.$$

- The second order derivative

$$\nabla^2 f=\left(\vec{b}\cdot\nabla\right)^2 f-\frac{\lambda}{\hat{g}}\kappa_g\vec{b}\cdot\nabla f-\vec{\kappa}\cdot\nabla f+\nabla_\perp^2 f, \tag{37}$$

where $\nabla_\perp^2 f=(\vec{e}_1\cdot\nabla)^2 f-\kappa_{nd}\vec{e}_1\cdot\nabla f+(\vec{e}_2\cdot\nabla)^2 f-\hat{g}\kappa_p\vec{e}_2\cdot\nabla f$.

- $\mathcal{K}(f)\equiv\nabla\cdot\left(\frac{\vec{B}\times\nabla f}{B^2}\right)=-2\vec{\kappa}\cdot\frac{\vec{B}\times\nabla f}{B^2}-\frac{|\nabla\rho|}{B}\frac{\mu_0 P'}{B^2}\vec{e}_2\cdot\nabla f$.

Contents

Flux function and flux surface average

- A variant which is only a function of magnetic flux is call **flux function**, such as $q(\psi)$, $g(\psi)$, $P(\psi)$, $T(\psi)$, and $N(\psi)$ etc.
- Some of the variants depend on the geometry of the flux surface, for example, R, B, and J_ϕ etc are all not flux function.
- In transport studies, the transport flux is often evaluated on each flux surface. It is necessary to do the **flux surface average** for those non-flux functions.
- Flux surface average in tokamak

$$\langle F\rangle_\psi = \frac{\oint_s F\mathcal{J}d\theta d\phi}{\oint_s \mathcal{J}d\theta d\phi} = \frac{\oint_l F\mathcal{J}d\theta}{\oint_l \mathcal{J}d\theta} = \frac{1}{2\pi\hat{V}'}\oint_l F\mathcal{J}d\theta = \frac{\oint_l F(dl/B_p)}{\oint_l (dl/B_p)} \tag{38}$$

where $\hat{V}' \equiv d\hat{V}/d\rho = \frac{1}{2\pi}\oint_l \mathcal{J}d\theta$. If $\rho = \rho_t$, then $\hat{V}' = \frac{\rho B_0}{g\langle 1/R^2\rangle_\psi}$.

- One important **flux surface average** term in **transport studies** [Hinton, **RMP 48**, 239 (1976)]

$$\left\langle\nabla\cdot\vec{F}\right\rangle_\psi = \left\langle\mathcal{J}^{-1}\partial_\rho(\mathcal{J}F^\rho)\right\rangle_\psi = \frac{\partial_\rho[\langle F^\rho\rangle_\psi \oint\mathcal{J}d\theta]}{\oint\mathcal{J}d\theta} = \frac{1}{\hat{V}'}\partial_\rho[\hat{V}'\langle F^\rho\rangle_\psi] \tag{39}$$

Flow decomposition in a toroidal configuration

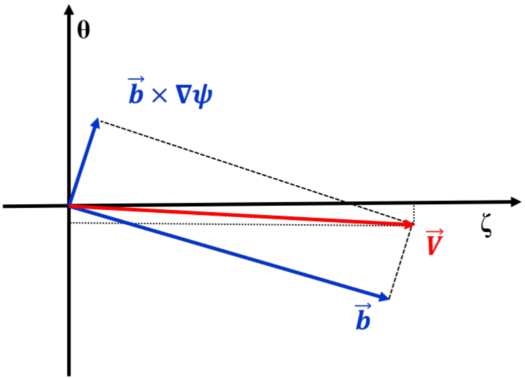

1.23 Vector decomposition

From geometric relation

$$\frac{1}{B}\vec{b}\times\nabla\psi_p = \frac{B_\zeta}{B}\vec{b} - e_\zeta, \tag{40}$$

it has

$$\begin{aligned}\vec{V} &= V_\parallel\vec{b} - \Omega_\perp(\psi)\frac{1}{B}\vec{b}\times\nabla\psi_p \\ &= \hat{\Omega}^\theta(\psi)\vec{B} + \Omega_\perp(\psi)e_\zeta, \end{aligned}\tag{41}$$

where

$$\hat{\Omega}_\theta \equiv \frac{V^\theta}{B^\theta} = \frac{V_\parallel}{B} - \frac{B_\zeta}{B^2}\Omega_\perp, \tag{42}$$

$$\Omega_\perp \equiv \Omega_E + \Omega_* \tag{43}$$

are flux functions [Sun, **NF 51**, 053015 (2011)]. Here $\Omega_E = -\frac{\mathrm{d}\Phi}{\mathrm{d}\psi_p}$ and $\Omega_* = -\frac{1}{Ne}\frac{\mathrm{d}P}{\mathrm{d}\psi_p}$ are $\vec{E}\times\vec{B}$ and diamagnetic drift frequency, respectively.

Toroidicity induced Pfirsch-Schlüter current

- From $B \propto \frac{1}{R}$, it has

$$B \approx B_0(1 - \epsilon \cos\theta). \tag{44}$$

- It is easy to obtain that

$$\sigma \equiv \frac{\mu_0 J_\parallel}{B} = -[\frac{g}{B^2}\mu_0 \frac{dP}{d\psi_p} + \frac{dg}{d\psi_p}], \tag{45}$$

  which is an important equilibrium property.

- let's write $\sigma = \bar{\sigma} + \sigma_{ps}$, it has $\bar{\sigma} \equiv \mu_0 \frac{\langle J_\parallel B\rangle_\psi}{\langle B^2\rangle_\psi}$ is the net parallel current and

$$\sigma_{ps} \equiv \frac{\mu_0 J_\parallel^{ps}}{B} = -\mu_0 g \left[\frac{1}{B^2} - \frac{1}{\langle B^2\rangle_\psi}\right] \frac{dP}{d\psi_p} \tag{46}$$

  is the so-called **Pfirsch-Schlüter** current. This is an important toroidal effect. It can be evaluated, after the equilibrium solution is obtained.

- **Neoclassical transport** in Pfirsch-Schlüter regime: $\Gamma \propto \left\langle \frac{1}{B^2} - \frac{1}{\langle B^2\rangle_\psi} \right\rangle_\psi \propto 2q^2$

∇B, toroidicity and curvature

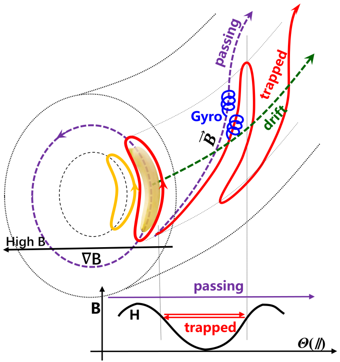

1.24 Particle orbits

Toroidicity ⇔ asymmetry of B in high and low field sides.

$$\nabla B = \vec{b}\left(\vec{b}\cdot\nabla B\right) + B\vec{\kappa} - \frac{\mu_0}{B}\nabla P. \quad (47)$$

- The first term on the RHS, i.e. $\vec{b}\cdot\nabla B$, produces the mirror field and causes **trapped** particles with banana orbit ($\rho_p \approx 2\sqrt{2}\frac{q}{\sqrt{\epsilon}}\rho_g$).
- $\nabla_\perp B$ or curvature causes the **drift** motion of guiding center. The toroidal drift frequency can be written as [Sun, **PoP 26**, 072504 (2019)]

$$\omega_B = -\left(\kappa_\rho - \frac{\mu_0 P'}{B^2}\right)\frac{\left(1+\xi^2\right)E}{e\psi_p'}. \quad (48)$$

- Driving term for **interchange and ballooning mode** [Connor, **PRL 40**, 396 (1978)] : $\propto -P'\kappa_\rho$
- Toroidicity induced parallel viscosity which causes the **damping of the poloidal flow** near the plasma core
- Electron parallel viscosity induces the **Bootstrapped current**

Equilibrium and geometric effects on stabilities

- Pressure gradient driving term

$$\delta W_F \propto \kappa_\rho \propto -\left[\cos\theta + \sin\theta\left(s\theta - \alpha_p \sin\theta\right)\right], \qquad (49)$$

where interchange mode driving $D_I = d_m \frac{\alpha_p}{s^2} - \frac{1}{4}$ with $d_m \propto -\left\langle \kappa_\rho \right\rangle_\psi$.

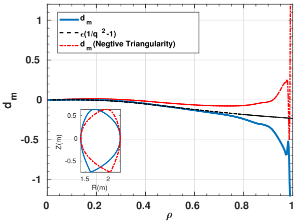

1.25 d_m [Sun, **AIP advances 14**, 055206 (2024)]

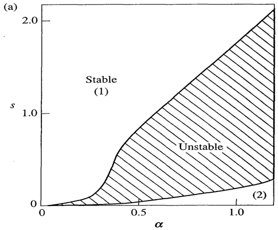

1.26 Second stability regime [Lortz, **PLA 68**, 49 (1978)]

- Toroidal precessional frequency

$$\langle\omega_B\rangle_b \propto -\left\langle \kappa_\rho \right\rangle_b$$

$$\approx \langle\cos\theta\rangle_b + s\,\langle\theta\sin\theta\rangle_b - \alpha_p \left\langle \sin^2\theta \right\rangle_b . \qquad (50)$$

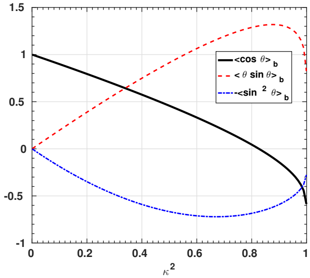

1.27 Precession

Equilibrium for operational scenario development

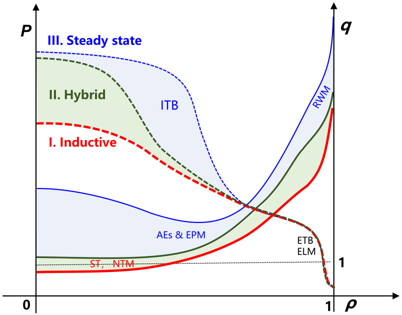

1.28 ITER operational Scenarios [Sun, **Acta Phys. Sin. 73**, 175202 (2024)]

- **Global MHD stabilities**
  - $q_{95} = \frac{aB}{I}S$ have a strong influence on the global **MHD β limit**
  - $\beta_N^{crit} = 4l_i \Rightarrow$ Global MHD stability depends on **current density** and **pressure** profiles
  - **Curvature** couples the global **MHD modes** driven by current density and pressure gradients
  - Toroidal and shaping effects create **gap modes** e.g. TAE mode
- **Micro-instabilities and transport**
  - Global **magnetic shear** s has stabilization effect on interchange mode
  - The **second stability** regime of ballooning mode is linked to the increase of the **local magnetic shear** (α_p effect in $\bar{\Lambda}_0$ and κ_ρ) in weak global shear case
  - **Geodesic curvature** couples the ion sound wave and Alfvén wave forming Geodesic Acoustic Mode (GAM) or Beta induced Alfvén Eigenmode (BAE) *etc*

Contents

Curvilinear coordinates

- The Jacobian for coordinate transfrom from Cartesian coordinates (x, y, z) to a **curvilinear coordinates** (α, β, γ) is defined as
$$\mathcal{J} \equiv \frac{\partial(x, y, z)}{\partial(\alpha, \beta, \gamma)} = [(\nabla\alpha \times \nabla\beta) \cdot \nabla\gamma]^{-1} \quad (51)$$
The differential volume can be written as $dV = dxdydz = \mathcal{J} d\alpha d\beta d\gamma$.
- **Contravariant** base vectors
$$(e^\alpha, e^\beta, e^\gamma) \equiv (\nabla\alpha, \nabla\beta, \nabla\gamma), \quad (52)$$
and **covariant** base vectors
$$(e_\alpha, e_\beta, e_\gamma) \equiv (\partial_\alpha \vec{X}, \partial_\beta \vec{X}, \partial_\gamma \vec{X}) = \mathcal{J}(\nabla\beta \times \nabla\gamma, \nabla\gamma \times \nabla\alpha, \nabla\alpha \times \nabla\beta). \quad (53)$$
It has $e^i \cdot e_j = \delta_{ij}$, and $e_\alpha \times e_\beta = \mathcal{J} e^\gamma$.

Geometric meaning of the Curvilinear coordinates

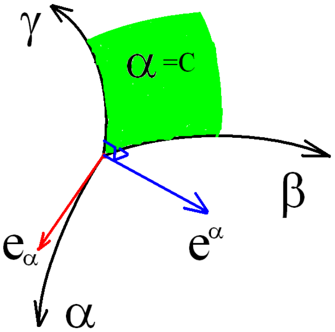

1.29 Geometric meaning of the Curvilinear coordinates

- $(\alpha = const, \beta = const, \gamma = const)$ are the **coordinate surfaces.**
- (α, β, γ) are the **coordinate lines.**
- The contravariant coordinates $(e^\alpha, e^\beta, e^\gamma) \equiv (\nabla\alpha, \nabla\beta, \nabla\gamma)$ are **normal** to the coordinate surfaces
- The covariant coordinates $(e_\alpha, e_\beta, e_\gamma)$ are **tangential** to the coordinate lines.

Metrics

- The metrics of the coordinates are defined as: $g^{\alpha\beta} = e^{\alpha} \cdot e^{\beta}$ and $g_{\alpha\beta} = e_{\alpha} \cdot e_{\beta}$.
- It has $g_{ij}g^{jk} = \delta_{ik}$ (two j means summary over all the coordinates, this will also be used as default in the following) and $e_i = g_{ij}e^j$.
- The relationship between the metrics and the Jacobian can be written as

$$det(g^{ij}) = 1/\mathcal{J}^2 \quad and \quad det(g_{ij}) = \mathcal{J}^2 \tag{54}$$

- The covariant of the metrics can be calculated from the contravariant of the metrics with

$$g_{\alpha\alpha} = \mathcal{J}^2[g^{\beta\beta}g^{\gamma\gamma} - (g^{\beta\gamma})^2] \tag{55a}$$

$$g_{\alpha\beta} = \mathcal{J}^2[g^{\alpha\gamma}g^{\beta\gamma} - g^{\alpha\beta}g^{\gamma\gamma}] \tag{55b}$$

Metrics evaluation for flux coordinates

All the metrics $g^{\alpha\beta}$ (contra-variants), $g_{\alpha\beta}$ (co-variants) can be written as a combination of $g^{\rho\rho}, g^{\rho\theta}, g^{\theta\theta}$.
The basic metrics $g^{\rho\rho}$, $g^{\rho\theta}$ and $g^{\theta\theta}$ can be calculated from the following equations

$$g^{\rho\rho} = \left(\frac{R}{\mathcal{J}}\right)^2 [(\partial_\theta R)^2 + (\partial_\theta Z)^2] \quad (56)$$

$$g^{\rho\theta} = -\left(\frac{R}{\mathcal{J}}\right)^2 [\partial_\rho R \partial_\theta R + \partial_\rho Z \partial_\theta Z] \quad (57)$$

$$g^{\theta\theta} = [(g^{\rho\theta})^2 + R^2/\mathcal{J}^2]/g^{\rho\rho} \quad (58)$$

The covariants of the metric can be transformed form the contravariant ones by using their definitions.

Other useful formulas

- Some other useful identities about operators:

$$\nabla \times \nabla f = 0 \tag{59a}$$

$$\nabla \cdot (\nabla f \times \nabla g) = 0 \tag{59b}$$

$$\nabla \cdot (\vec{A} \times \vec{B}) = \vec{B} \cdot \nabla \times \vec{A} - \vec{A} \cdot \nabla \times \vec{B} \tag{59c}$$

$$\nabla \times (\vec{A} \times \vec{B}) = [\nabla \cdot \vec{B} + \vec{B} \cdot \nabla]\vec{A} - [\nabla \cdot \vec{A} + \vec{A} \cdot \nabla]\vec{B} \tag{59d}$$

$$\vec{A} \times (\nabla \times \vec{B}) = (\nabla \vec{B}) \cdot \vec{A} - (\vec{A} \cdot \nabla)\vec{B} \tag{59e}$$

$$\nabla(\vec{A} \cdot \vec{B}) = \vec{A} \times (\nabla \times \vec{B}) + \vec{B} \times (\nabla \times \vec{A}) \tag{59f}$$

$$+(\vec{A} \cdot \nabla)\vec{B} + (\vec{B} \cdot \nabla)\vec{A} \tag{59g}$$

$$\nabla^2 \vec{A} = \nabla(\nabla \cdot \vec{A}) - \nabla \times (\nabla \times \vec{A}) \tag{59h}$$

$$\nabla \cdot (\vec{A}\vec{B}) = (\nabla \cdot \vec{A})\vec{B} + (\vec{A} \cdot \nabla)\vec{B} \tag{59i}$$

$$\oint_v \nabla \cdot \vec{A} dv = \oint_s \vec{A} \cdot d\vec{s} \tag{59j}$$

$$\oint_s \nabla \times \vec{A} \cdot d\vec{s} = \oint_l \vec{A} \cdot d\vec{l} \tag{59k}$$